Nuclear Instruments and Methods in Physics Research A 368 (1996) 635-639

NUCLEAR INSTRUMENTS & METHODS IN PHYSICS RESEARCH Section A

# Ionization chamber as a p, d and $\alpha$ beam intensity monitor

Y. Sugaya [a], Y. Yamanoi [b], J. Chiba [b], Yu. Kiselev [c], M. Numajiri [b], H. Ochiishi [d], K.H. Tanaka [b], K. Yasuda [e], Y. Yoshimura [b,*]

[a] Tokyo University of Agriculture and Technology, Tokyo, Japan
[b] National Laboratory for High Energy Physics (KEK), Tsukuba, Japan
[c] Institute of Theoretical and Experimental Physics, Moscow, Russian Federation
[d] Department of Physics, Kyushu University, Fukuoka, Japan
[e] Department of Physics, Kyoto University, Kyoto, Japan

Received 16 May 1995; revised form received 14 August 1995

**Abstract**

An ionization chamber was studied as a low-intensity beam monitor and worked well for p, d and $\alpha$ beams in the intensity range from $2.0 \times 10^6$ to $1.4 \times 10^{12}$ particles per 1.5 second spill. The stability of response to beams was within 2% during 3 weeks of measurements of subthreshold $\bar{p}$ production.

## 1. Introduction

A beam intensity monitor of the ionization chamber type was first made thirty years ago, and simple chambers are still being used for low-intensity beams at BNL [1], CERN [2] and JINR [3]. However, their performance has never been reported in detail.

At the proton synchrotron of the National Laboratory for High Energy Physics (KEK-PS), many secondary emission chambers [4,5] are normally used to monitor the proton beam, being calibrated by an activation method. However, because of a poor S/N ratio, a secondary emission chamber can't be used for a beam intensity lower than $10^9$ pps (particles per spill, the spill width is about 1.5 s). In addition, the response is not clearly known for deuteron or $\alpha$ beams. The ionization chamber can bridge the gap between a scintillation counter and a secondary emission chamber in the region from $10^6$ to $10^9$ pps, since the charge yield from an ionization chamber is much higher than that of a secondary emission chamber, and its output signal can be easily discriminated from noise. After calibration for proton beams, the ionization chamber was used as the intensity monitor for deuteron and $\alpha$ beams in an experiment of subthreshold $\bar{p}$ production [6] at the KEK-PS, since the charge yield is nearly proportional to the square of the charge of incident beams in the KEK-PS energy region.

The characteristics of primary beams at the KEK-PS are mentioned in Table 1.

Table 1
Characteristics of primary beams

| | |
|---|---|
| Energy | 2~12 GeV for proton beams |
| | 1~5.6 GeV/nucleon for deuteron and $\alpha$ beams |
| Typical intensity | $4 \times 10^{12}$ pps for proton beams |
| | $2 \times 10^{12}$ pps for deuteron beams |
| | $5 \times 10^{10}$ pps for $\alpha$ beams |
| Spill | 1.5 s with a 4 s repetition period |
| Size | <1 cm (FWHM) |

## 2. Construction

The ionization chamber described in this paper is illustrated in Fig. 1. Three kinds of electrode assemblies were made: 21 electrodes with a 4 mm gap, 11 electrodes with a 4 mm gap and 11 electrodes with an 8 mm gap. The active lengths of the ionization chambers were thus 8 cm and 4 cm. The electrodes were made of aluminum foil (7 $\mu$m thick and 10 cm in diameter), which were supported with a 1 mm thick aluminum frame. These electrodes were connected alternately, with negative high voltage applied to the odd numbered electrodes and the signal read-out from the even numbered electrodes. The electrode assembly was placed in an aluminum container with two beam windows made of polyimide film (0.125 mm thick). The assembly was isolated from the container and shielded electrically with an aluminum cover in order to reduce noise, as shown in Fig. 1. After evacuating to 0.03 Pa for 1 day, the chamber ($4\ell$) was filled with pure argon gas to either 1.05 atm ($1.06 \times 10^5$ Pa) or 1.08 atm ($1.09 \times 10^5$ Pa), and then sealed for beam-intensity measurements. A pressure slightly higher than atmosphere was used to keep a positive pressure on the

* Corresponding author.

0168-9002/96/$15.00 © 1996 Elsevier Science B.V. All rights reserved
SSDI 0168-9002(95)00844-6

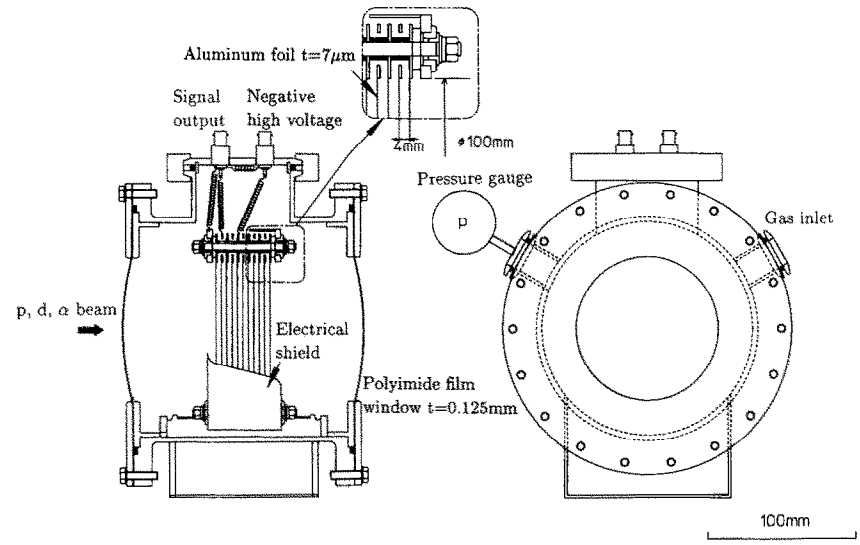


Fig. 1. Illustration of an ionization chamber with 11 electrodes having a 4 mm gap.

beam windows.

Electrons from ionized argon were collected at the electrodes, and the charge was read-out by a current digitizer (EG&G-ESN CD1010).

## 3. Performance test

The range of the beam intensity which can be measured by the ionization chamber is restricted by the drop of the effective applied voltage caused by argon ions in the inter-electrode gap. When $N$ ion pairs per $cm^3$ per sec are produced by beams, the voltage drop, $V_{ion}$, is given by

$$V_{ion} = \frac{1}{\sqrt{4\varepsilon\mu_+}}\sqrt{eN}\,d^2 \qquad (1)$$

according to Ref. [7]. Here $e$ is the electron charge (C), $\mu_+$ the mobility of the argon ions ($cm^2 s^{-1} V^{-1}$), $d$ the electrode spacing (cm) and $\varepsilon$ the permittivity of the gas ($C V^{-1} cm^{-1}$). To collect all of the electrons, a negative voltage higher than $V_{ion}$ must be applied to the gaps.

In order to see the performance described by Eq. (1), the response current was measured at different values of $d$ and $N$. $\beta$-rays ($^{90}Sr$, $2\times10^6$ Bq) were used as ionizing particles, and injected through the beam window. Fig. 2 shows the measured response curves as a function of the applied voltage. Space charge effects of the argon ions prevent one from efficiently collecting electrons at a lower applied voltage. The current increases and becomes saturated as one collects almost all of the electrons at a certain value of voltage. It appears from the curves that the saturated current becomes larger for higher pressure, although they are not proportionally correct due to path length variations and multiple scattering of the uncollimated $\beta$ rays. Curves of current versus electrode spacing ($d$) also showed a similar feature.

After testing with a $\beta$ source, the 4 mm gap ionization chamber was installed in the beam line. The charge per spill was measured as a function of the applied voltage for 12 GeV proton beams at beam intensities of $7\times10^{10}$ pps and $2\times10^{11}$ pps, and compared with the value from a secondary emission chamber (Fig. 3). It can be seen that the applied voltages of 250 V and 400 V are sufficient to collect almost all of the electrons produced by proton beams of $7\times10^{10}$ pps and $2\times10^{11}$ pps, respectively. We defined this applied voltage as the saturation voltage ($V_{sat}$). Since $V_{ion}$ has been estimated by Eq. (1) to be 210 V for an intensity of $2\times10^{11}$ pps, $V_{sat}$ is a few times higher than $V_{ion}$. Such a high applied voltage minimizes recombination loss, since most of the argon ion is swept out and the electron drift ve-

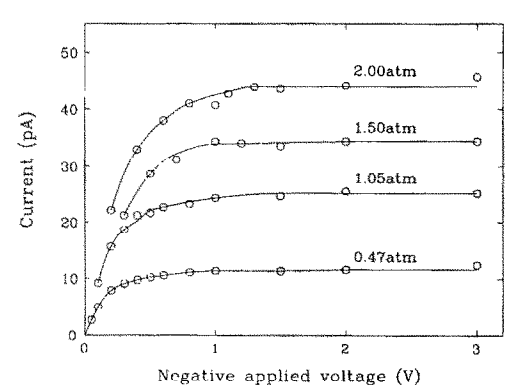


Fig. 2. Response curves for the $^{90}Sr$ $\beta$-ray source at various gas pressures. The horizontal axis is the applied voltage and the vertical is current from the ionization chamber. The lines are eye-guides.

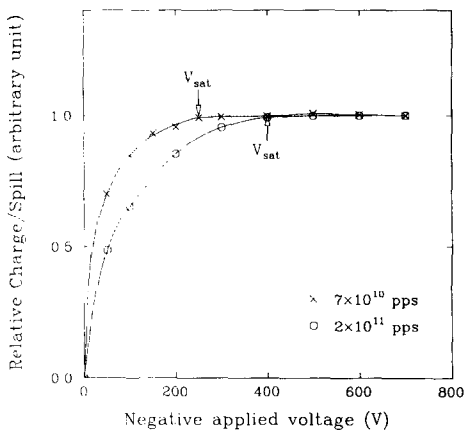


Fig. 3. Charge yield from a 4 mm gap chamber at proton intensities of $7 \times 10^{10}$ pps and $2 \times 10^{11}$ pps. The horizontal axis is the applied voltage and the vertical is the charge per spill. The number of protons per spill was measured by a secondary emission chamber.

locity increases. The saturation voltage as function of beam intensity is given in Fig. 4, together with that for an 8 mm gap electrode assembly. Since the beam intensity fluctuates spill by spill, each point has an error of ±15% in the intensity and the saturation voltage. In this figure, it may be seen that the $V_{sat}$ is proportional to the square root of the beam intensity, as expected from Eq. (1).

The applied voltage should be set at the point higher than the saturation voltage, corresponding to the highest beam intensity foreseen in an experiment. In other words, the measurements with these ionization chambers at high intensities are limited by whether or not the break-down voltage is higher than the saturation voltage. An ionization chamber with an 8 mm gap has a break-down voltage of 1800 V, and one with a 4 mm gap has one at 1000 V. However, the 4 mm gap chamber has an advantage at a higher intensity beam, because the ratio of saturation voltages ($\sim\frac{1}{3}$ in Fig. 3) is also expected to be lower than the ratio of break down voltages (1000 V/1800 V).

Intensity measurements for 12 GeV proton beams were carried out using the 4 mm gap ionization chambers with an active length of 4 cm and 8 cm. The gas filling pressures were 1.08 atm and 1.05 atm, and the applied voltages were mainly 1000 V and 50 V, respectively. The former was installed in the EP2 beam line for higher intensity beams ($\sim 10^{12}$ pps) and the latter was installed in the P1 beam line for lower intensity beams ($10^6 \sim 10^{10}$ pps). In Fig. 5 the charge from the ionization chamber, $Q_{IC}$, is plotted as a function of the beam intensity, as measured by a secondary emission chamber or a scintillation counter ($<5 \times 10^6$ pps). The charge is normalized to an effective length of 1 cm and a gas filling pressure of 1.0 atm. The linearity of the charge versus the beam intensity was confirmed for proton beams up to $2.5 \times 10^{11}$ pps, and data points were to within 12% (RMS). Deuteron and $\alpha$ beams were measured later, and those data are also plotted on the line with a deviation of 10% (RMS) up to $1.4 \times 10^{12}$ pps (Fig. 5).

When $N_p$ protons pass through the ionization chamber, the conversion factor from the output charge to the beam intensity, $N_p/Q_{IC}$, was obtained for 12 GeV protons, comparing to that from the secondary emission chambers which were already calibrated by an activation method. The conversion

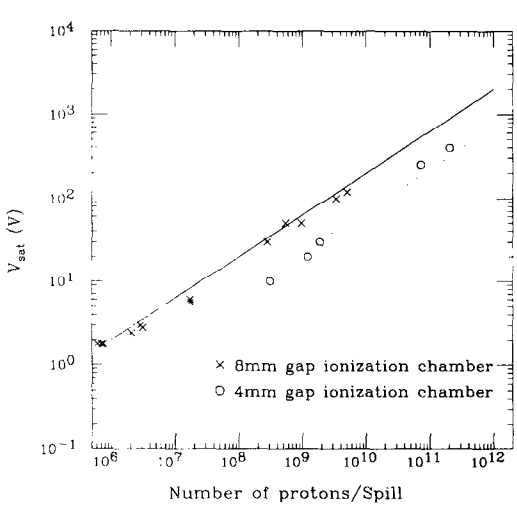


Fig. 4. $V_{sat}$ measured with the proton beam. The horizontal axis is the beam intensity measured by the secondary emission chamber. The dotted line indicates the square root of the intensity, as measured using a 4 mm gap ionization chamber. The solid line is that for an 8 mm gap ionization chamber.

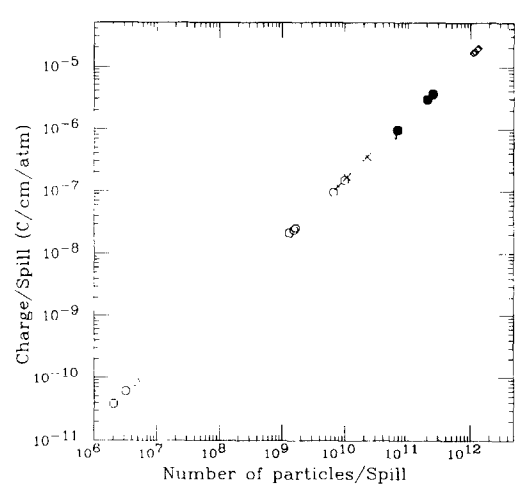


Fig. 5. The charge from ionization chambers for p, d and $\alpha$ beams. Symbols of •, ◇ and × indicate the charge from the 4 cm ionization chamber for p, d and $\alpha$ beams. The charge for the $\alpha$ beam is divided by 4. The symbol of ○ indicates the charge from an 8 cm chamber for the p beam. The energy is 12 GeV for protons and 5.0, 4.0 and 3.0 GeV/nucleon for deuteron and $\alpha$ beams. The number of particles was measured by a secondary emission chamber or a scintillation counter.

factors of the ionization chambers with effective lengths of a 4 cm and an 8 cm were obtained to be $1.6 \times 10^{16}$ proton/C and $0.78 \times 10^{16}$ proton/C at intensities of $2 \times 10^{11}$ pps and $2 \times 10^{9}$ pps, respectively. The error in the conversion factors came mainly from the activation method used to calibrate the secondary emission chamber, and the value was about 10%. From these conversion factors, the number of ion pairs produced in argon gas by a particle, $N_{pair}$, can be estimated by the following equation:

$$N_{pair} = \frac{1}{e\ell P}\frac{Q_{IC}}{N_p}, \tag{2}$$

where $\ell$ is the effective length (4 cm or 8 cm), and $e$ is the electron charge ($1.6 \times 10^{-19}$ C). $P$ is the pressure of argon gas (1.08 atm or 1.05 atm). $N_{pair}$ for a 12 GeV proton was measured to be 90 and 96 per cm for the 4 cm and 8 cm ionization chambers, respectively. It is known that about 94 ion pair are produced when a minimum ionizing particle passes through 1 cm in 1 atm of Argon gas [8]. Although $N_{pair}$ for a 12 GeV proton is about 10% higher than that of a minimum ionizing particle due to a relativistic rise [9], the measured values of $N_{pair}$ are consistent with this value, taking into account the error in the conversion factor.

## 4. Response to deuteron and $\alpha$ beams

In the experiment of subthreshold $\bar{p}$ production [6], the intensity of $\alpha$ beams was measured by two kinds of detectors (an ionization chamber and a secondary emission chamber) and was confirmed by two kinds of calibration methods (the pion-production and activation methods [10]). The charge in the ionization chamber and the secondary emission chamber originate from electromagnetic interactions between beam particles and material. Therefore, the charge for $\alpha$ beams is expected to be about four-times higher than that for the proton beams. In order to confirm whether or not the measured intensity of $\alpha$ beams was consistent with each other, a cross-check was made among the above four methods.

An activation method of calibration was performed by exposing aluminum foil to $\alpha$ beams of 2.0, 3.0 and 5.0 GeV/nucleon for 20 minutes. The experimental cross sections of the reaction which can be used in this activation method are given in Table 2. The cross sections used for the present estimation of the $\alpha$-beam intensity are 42.0 mb for $^{12}C(\alpha,\alpha n)^{11}C$, 16.3 mb for $^{12}C(\alpha,sp)^{7}Be$ and 22 mb for $^{27}Al(\alpha,sp)^{24}Na$. The error in this activation method is about 12%, which comes mainly from the above reaction cross sections. The intensity of $\alpha$ beams measured by this activation method and the ionization chamber is given in Table 3, being divided by that from the secondary emission chamber. The errors are about 16%, including those from the calibration of the secondary emission chamber(10%). By compensating the charge ratio, the conversion factor for 12 GeV proton beams is used for the ionization chamber and the secondary emission chamber. But the energies of $\alpha$ beams in this activation method were 5.0, 4.0 and 3.0 GeV/nucleon. An energy deposit from a particle to the secondary emission chamber depends on its energy. The energy deposit of a 12 GeV proton is about 10% higher than that of a 5.0~3.0 GeV/nucleon particle due to relativistic rise. Therefore, the ratio of the number of $\alpha$ particles from the activation method and from the secondary emission chamber should be 10% smaller than the value in Table 3. The differences in Table 3 for the $\alpha$ beam are within tolerance considering the large errors from the activation method for $\alpha$ beam and the calibration of the secondary emission chamber.

Table 2
Experimental cross sections of an $\alpha$-induced reaction which can be used in an activation method of calibration

| Mode | Energy (GeV/nucleon) | $\sigma_{tot}$ (mb) | Ref. |
|---|---|---|---|
| $^{12}C(\alpha,\alpha n)^{11}C$ | 0.3 | 49.2±1.9 | [11] |
| | 0.3975 | 46.4±1.3 | [12] |
| | 0.5 | 44.1±1.8 | [11] |
| | 0.7 | 42.0±1.7 | [11] |
| | 1.0475 | 42.5±1.1 | [12] |
| | 2. | 43.±3. | [13] |
| | 3.65 | 42.0±0.7 | [14] |
| $^{12}C(\alpha,sp)^{7}Be$ | 0.3 | 19. | [15] |
| | 0.7 | 16.3±1.5 | [16] |
| | 1.15 | 16.3 | [17] |
| $^{27}Al(\alpha,sp)^{24}Na$ | 0.095~0.1025 | 24.2±0.3 | [18] |
| | 0.15 | 19.7±2.4 | [18] |
| | 0.18 | 20.9±2. | [18] |
| | 0.225~0.23 | 22.0±2.0 | [18] |

The pion production cross sections in the proton-carbon reaction and the $\alpha$-carbon reaction were used to check the response of the ionization chamber. Assuming that a nucleon in an $\alpha$ particle produces a pion independently, and that the charge-conjugation relation,

$$\sigma(p + C \rightarrow \pi^+ + X) = \sigma(n + C \rightarrow \pi^- + X), \tag{3}$$

is correct, the pion production cross section in the $\alpha$-carbon reaction can be given as

$$\sigma(\alpha + C \rightarrow \pi^- + X) = 2 \times \left[\sigma(p + C \rightarrow \pi^- + X) + \sigma(p + C \rightarrow \pi^+ + X)\right]. \tag{4}$$

Table 3
$\alpha$ beam intensity ratios as measured by activation and the ionization chambers, as compared with that for the secondary emission chambers

| Energy (GeV/nucleon) | 5.0 | 3.0 | 2.0 |
|---|---|---|---|
| $N_{acti}(^{11}C)/N_{SEC}$ | 0.93 | 0.98 | 0.96 |
| $N_{acti}(^{7}Be)/N_{SEC}$ | 1.13 | 1.04 | 1.03 |
| $N_{acti}(^{24}Na)/N_{SEC}$ | 0.85 | 0.87 | - |
| $N_{IC}/N_{SEC}$ | 1.03 | 1.01 | 1.04 |

Table 4
$\pi$ production cross sections (mb/sr/(GeV/$c$)) measured in the proton-carbon and $\alpha$-carbon reactions. The beam energy is 5.0 GeV/nucleon and the production angle is 5.1°. The intensity of proton and $\alpha$ beams was measured by the secondary emission chamber and the ionization chamber, respectively

| $\pi$ momentum (GeV/$c$) | 1.0 | 1.5 | 2.0 | 2.5 |
|---|---|---|---|---|
| {1} $\frac{d^2\sigma}{dp\,d\Omega}(p + C \rightarrow \pi^- + X)$ | 95.6 | 74.3 | 42.4 | 23.5 |
| {2} $\frac{d^2\sigma}{dp\,d\Omega}(p + C \rightarrow \pi^+ + X)$ | 186.1 | 210.5 | 133.3 | 67.2 |
| $2 \times (\{1\} + \{2\})$ | 563.4 | 569.6 | 351.4 | 181.4 |
| $\frac{d^2\sigma}{dp\,d\Omega}(\alpha + C \rightarrow \pi^- + X)$ | 579.1 | 540.9 | 333.8 | 158.4 |

The pion production cross sections taken during the experiment of the subthreshold $\bar{p}$ production are shown in Table 4. The beam energy was 5.0 GeV/nucleon and the production angle was 5.1°. For the cross section of $\alpha$-induced reactions, the beam intensity was measured by the ionization chamber. The systematic error in these cross section measurements is estimated to be 12%, and the statistical error is less than 1%. The difference between the measured $\alpha$-induced cross sections and those estimated by Eq. (4) is within this error.

The charge yield of the ionization chamber for $\alpha$ beams is divided by 4 and plotted in Fig. 5. The deuteron beam intensity was also measured by the ionization chamber and secondary emission chamber and plotted in Fig. 5. The response of the secondary emission chamber for deuteron beams had been previously confirmed to be the same as for proton beams [5]. Data from deuteron beams and $\alpha$ beams are in line with the response for proton beams, with a deviation of 10%.

An ionization chamber, which was sealed off from the gas system, was operated stably for $\alpha$ beams, and variation in the charge yield including readout electronics were within 2% during 3 weeks of experiment of subthreshold $\bar{p}$ production (Fig. 6).

## 5. Conclusion

Ionization chambers were studied for the purpose of measuring the intensity of p, d and $\alpha$ beams. The saturation voltage (or the voltage drop) is proportional to the square root of the beam intensity, as expected by Eq. (1). The upper end of the measurement range of the beam intensity is restricted by the fact that the saturation voltage should not be higher than break-down voltage. The linearity of charge yield for p, d and $\alpha$ beams was confirmed to be within 10%, compared with the values measured by a secondary emission chamber and a scintillation counter in the range of intensities from $2.0 \times 10^6$ to $1.4 \times 10^{12}$ pps. The charge yield from the ionization chamber was proportional to square of the particle's charge to within 10%. This fact was also confirmed for the deuteron and $\alpha$ beam measurements by an activation method and a measurement of the pion production cross section. Absolute values for the number of ion pairs in the conversion factor also has the error of 10% for this activation method.

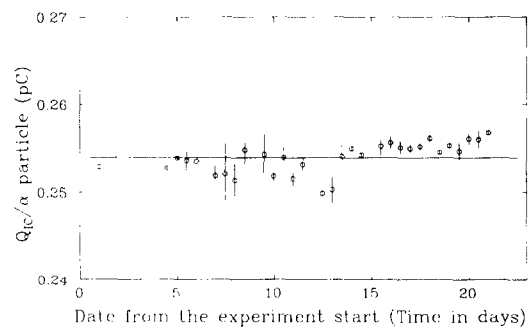


Fig. 6. Stability response of an ionization chamber for $\alpha$ beams during three weeks of operation. The vertical axis is the charge from the ionization chamber per $\alpha$ particle. The horizontal axis indicates the date from the experiment start. Data in a half day are averaged in one bin, and error bar shows RMS of the data in a half day. The solid line shows the mean value of all data. The dotted lines show the deviation of ±2% from the mean value.

## Acknowledgements

We would like to thank Dr. T. Miura for intensity measurements using an activation method. We also wish to thank the beam-channel group of the KEK-PS, and especially Prof. M. Takasaki, for their support. We would like to also thank members of the APEX collaboration for help during this work. A part of this work was supported by a Grand-in-Aid for Scientific Research (c) (No. 06640423) of the Japan Ministry of Education, Science and Culture (Monbusho).

## References

[1] G. Levine et al., Rev. Sci. Instr. 34 (1963) 1398.
[2] V. Agroitsas, Nucl. Sci. NS-28 (1981) 2243.
[3] M. Zielenski and A.L. Shishkin, JINR P13-88-142.
[4] H. Hirabayashi et al., J. Phys. Soc. Jpn. 51 (1982) 3098.
[5] M. Ieiri et al., Proc. 9th Symp. on Accelerator Science and Technology (1993) 477.
[6] J. Chiba et al., Nucl. Phys. A 583 (1995) 633.
[7] J. Sharpe, "Nuclear Radiation Detector", W.S. Cowell, Ltd.
[8] F. Sauli, CERN 77-09 (1977).
[9] D. Jeanne et al., Nucl. Instr. and Meth. 111 (1973) 287.
[10] M. Numajiri, private communication.
[11] J.R. Radin et al., Phys. Rev. C 26 (1982) 2565.
[12] V. Geaga et al., Nucl. Phys. A 386 (1982) 589.
[13] V. Geaga et al., Phys. Rev. Lett. 45 (1980) 1993.
[14] P. Kozma et al., JINR Report E1-89-745 (Dubna, 1989).
[15] G.M. Raisbeck et al., Spallation Nuclear Reactions and Their Applications (Reidel, Dordrecht, 1976) 83 p.
[16] G.M. Raisbeck et al., Phys. Rev. Lett. 35 (1975) 155.
[17] G.M. Raisbeck et al., Proc. 14th Int. Cosmic Ray Conf. (Munich, Germany, 1975), O.G.9.2-3.
[18] P. Karol, Phys. Rev. C 10 (1974) 150.